Tổng hợp vật liệu composite g-C_3N_4/ZnO tăng cường hoạt tính quang xúc tác dưới ánh sáng khả kiến

TÓM TẮT

Trong nghiên cứu này, vật liệu composite ZnO/g-C_3N_4 đã được tổng hợp thành công bằng phương pháp nung đơn giản từ các tiền chất g-C_3N_4 và zinc acetate hexahydrate. Hoạt tính quang xúc tác của vật liệu được đánh giá qua sự phân hủy dung dịch thuốc nhuôm rhodamine B (RhB) dưới ánh sáng nhìn thấy. Hình thái, độ kết tinh, thuộc tính hình học và liên kết hóa học của vật liệu được đặc trưng bằng các kỹ thuật phân tích khác nhau như hiển vi điện tử quét (SEM), nhiễu xạ tia X (XRD), phổ phản xạ khuếch tán tử ngoại khả kiến (UV-Vis DRS), phổ hồng ngoại (FT-IR). Kết quả cho thấy thuộc tính quang xúc tác của vật liệu composite phân hủy dung dịch thuốc nhuôm RhB cao hơn các vật liệu đơn ZnO, g-C_3N_4. Phản ứng phân hủy tuân theo mô hình động học bậc nhất với hằng số tốc độ phản ứng là 0.0243 phút^{-1}, gấp hơn hai lần so với g-C_3N_4 tinh khiết (0.0091 phút^{-1}).

Từ khóa: *g-C_3N_4, ZnO, composite, hoạt tính quang xúc tác, rhodamine B*

A facile synthesis of g-C_3N_4/ZnO composite with enhanced visible light photocatalytic activity

ABSTRACT

In this study, the ZnO/g-C_3N_4 composite was successfully synthesized using a facile calcination method with g-C_3N_4 and zinc acetate hexahydrate as the precursors. The photocatalytic activity of the synthesized composite was evaluated in the degradation of rhodamine B (RhB) under visible light. The morphology, crystallinity, optical properties, and chemical bond characteristics of the synthesized composite were characterized by using various analytical techniques such as scanning electron microscopy (SEM), Fourier-transform infrared (FTIR) spectroscopy, X-ray powder diffraction (XRD), ultraviolet-visible diffuse reflectance spectroscopy (UV-Vis DRS). The results showed that the photocatalytic properties of the composite were better than those of ZnO or g-C_3N_4 pristine. The degradation reaction follows a first-order kinetic model with a rate constant of 0.0243 min^{-1}, two times higher than g-C_3N_4 pristine (0.0091 min^{-1}). The synthesized composite was highly influential in the photocatalytic degradation of rhodamine B dye.

Keywords: *g-C_3N_4, ZnO, composite, photocatalytic activity, rhodamine B.*

1. INTRODUCTION

Removing pollutants from the textile industry through photocatalytic reaction has drawn increasing attention over the last few decades [1]. Recently, among advanced oxidation processes applied for organic pollutant degradation, photocatalysis has attracted much attention due to its utilization of solar radiation as a green energy source and oxygen in the air as an abundant oxidant. Consequently, various available oxide semiconductors, such as TiO_2, SiO_2, SnO_2, etc., have been widely investigated. However, besides their advantages in low economic and environmental cost suitable redox potential, the weaknesses, mainly activated by ultraviolet irradiation and high recombination rate of photo-induced charge carriers, limit their practical application. Therefore, it is necessary to search for alternatives with reasonable band structures for acceptable photocatalytic performance in visible light regions [2].

Zinc oxide (ZnO) is a promising photocatalyst for degrading organic and inorganic pollutants in wastewater due to its low price, nontoxicity, chemical stability, and high photocatalytic activity [3, 4, 5]. However, the photocatalyst ZnO has a large band gap of ~3.2 eV and absorbs only in the ultraviolet region. ZnO has almost no activity in the visible area [6]. It is an excellent strategy to prepare a composite with two photocatalysts by suitable matching band-level positions to decrease the electron−hole pair recombination [7].

Recently, graphite-like carbon nitride (g-C_3N_4) has attracted considerable attention as a potential visible light photocatalyst in water photo-splitting and organic pollutant degradation, which possesses very high thermal and chemical stability and interesting electronic properties. The metal-free polymeric photocatalyst g-C_3N_4 is considered a sensitizer candidate, possessing several advantages over other photocatalysts [5]. However, g-C_3N_4 insufficiently utilizes light, has a limited surface area, and yields a quick photoexcited electron-hole recombination rate, so it is limited by its poor photocatalytic ability [8]. To address these weaknesses, researchers applied critical scientific solutions, such as element doping into g-C_3N_4 [9] and preparing g-C_3N_4 composites with other semiconductors (metal sulfide [10], metallic oxide [11], and graphene category [12, 13]).

Several reports have been on the preparation of ZnO/g-C_3N_4 with different methods and have been used in many various applications. Renuka et al. synthesized g-C_3N_4/ZnO nanocomposite by co-precipitation method [14]. The photocatalytic efficiency of g-C_3N_4/ZnO nanocomposite (H = 93%) is higher than that of ZnO (H = 78%) and g-C_3N_4 single (H = 83%) with bisphenol A degradation in the UV light at pH = 6.5. Renathung et al. synthesized ZnO/g-

C_3N_4 nanocomposite by hydrothermal process [15]. The photodegradation of methylene blue could get 98% in ZnO/g-C_3N_4 nanocomposite, which could be attributed to the effective separation of photo-induced charge carriers between ZnO and g-C_3N_4.

In this study, the ZnO/g-C_3N_4 composite was synthesized by a simple calcination method, and its photocatalytic efficiency was determined through the degradation of RhB under visible light.

2. EXPERIMENTAL SECTION

2.1. Material synthesis

Chemicals: All the chemicals for materials synthesis, including zinc acetate dehydrate $Zn(CH_3COO)_2.2H_2O$ (99.5%), urea ($CO(NH_2)_2$, ≥99%), rhodamine B (RhB) were purchased from Merck and used directly without further purification

Materials synthesis:

The pure g-C_3N_4 was prepared by solid-state decomposition and condensation from urea as a precursor. Typically, a well-ground urea powder was transferred to an alumina crucible covered by an aluminum foil and then treated at 550 °C in the Argon gas for an hour with a temperature ramping of 10 °C·min^{-1}. The obtained solid product was re-grounded and denoted as g-C_3N_4.

The g-C_3N_4/ZnO was synthesized through the calcination facile method. Firstly, 100 mg of g-C_3N_4 was a mixture with 200 mg of zinc acetate dehydrate $Zn(CH_3COO)_2.2H_2O$. Next, the mixture was ground finely and calcined in the air at 350 ^oC for 1 hour. The solid was filtered, washed, and dried at 80 ^oC for 24 hours to obtain the composite product ZnO/g-C_3N_4 (denoted as ZCN). The material ZnO was also synthesized similarly to the above conditions but without g-C_3N_4 (marked as ZnO).

2.2. Material characterization

The phase structure information of the as-prepared samples was determined using X-ray diffraction spectra of the samples were measured on a Bruker D2 Advance diffractometer with a Cu X-ray tube with wavelength λ (CuKα) = 1.5406 Å, power 40 kV, current 40 mA. Scanning angle from 10 to 80^o. The Fourier-transform infrared (FT-IR) spectroscopy was carried out on an IRAffinity-1S spectrometer (Shimadzu) with wavenumbers ranging from 400 to 4000 cm^{-1}. The composition of the element was determined by EDS spectroscopy. UV-Vis-DRS spectra of material samples were determined on a Jasco-V770 machine with wavelengths from 200 - 800 nm. The morphology of the samples was investigated using field emission scanning electron microscopy (SEM) captured on Nova SEM 450.

2.3. Photocatalytic properties

The photocatalytic activity of the as-prepared samples was investigated in the degradation of RhB dye. As a typical procedure, 50 mg catalyst was dispersed in 100 mL of 10 mg.L^{-1} RhB solution. Then, the dispersion was kept in the dark under continuous stirring conditions for 60 min to achieve the adsorption-desorption equilibrium. In the next step, 150 µL of H_2O_2 30% solution was added. Finally, the dispersion was exposed to irradiation of a 30 W-LED lamp. For each interval of 20 min, 8 mL of dispersion was withdrawn and centrifuged to eliminate the solid. The RhB concentration was determined by measuring the intensity of the maximum absorption peak at a wavelength of 553 nm.

3. RESULTS AND DISCUSSION

3.1. Material characteristics

The XRD patterns of ZnO, g-C_3N_4, and ZCN composite are shown in Fig.1. The patterns show that the photocatalysts are well crystallized, the pure g-C_3N_4 sample has two distinct peaks at 12.87^o and 27.69^o, which are indexed for graphitic materials as the (100) and (002) [16]. The peak at 12.87^o represents stacking of aromatic units corresponding to the interplanar distance of 6.82 Å. The strong peak at 27.69^o is interlayer packing of aromatic tri-s-triazine with a stacking distance of 3.22 Å [17]. Meanwhile, the diffraction peaks at 2θ = 31.76^o, 34.44^o, 36.26^o, 47.56^0, 56.64^o, 62.94^o và 68.19^o in XRD patterns of ZnO, corresponding to the (100), (002), (101), (102), (110), (103) and (112) [18]. The XRD peaks of the pure ZnO sample agree with the hexagonal wurtzite structure (JCPDS No. 001-1136). The locus and shapes of characteristic peaks of ZCN are unchanged compared with those of pure ZnO. This demonstrated that modification with g-C_3N_4 does not affect ZnO's lattice structure, which is suitable for photocatalytic properties of as-prepared hybrid photocatalysts. As for a combination, the ZCN composites show the XRD patterns analogous to the XRD patterns of the components. The diffraction peaks of both ZnO and g-C_3N_4 phases are observable.

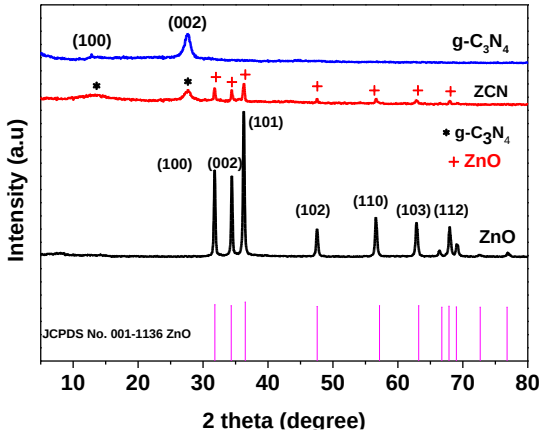

Fig. 1. XRD patterns of g-C_3N_4, ZnO, and ZCN.

The bond structure of ZnO, g-C_3N_4, and ZCN composite were analyzed by FT-IR measurement. Fig.2 show that the spectrum of g-C_3N_4 has found some strong band in the 1616 - 1200 cm^{-1} range, corresponding to typical stretching vibrations of C-N, C = N heterocycles [19]. The peak at 800 cm^{-1} was assigned to the s-triazine ring vibrations. While the peaks at 1616, 1560, 1461, and 1405 cm^{-1} were ascribed to stretching vibrations of heptazine-desired repeating units. The peak at 1313 and 1232 cm^{-1} belonged to the stretching vibration of connected trigonal units of C-N(-C)-C of bridging C-NH-C (partial condensation) [20]. Meanwhile, the broad absorption band 3300 - 3000 cm^{-1} and a small peak at 891 cm^{-1} can be ascribed to the N-H stretching vibrations and bend vibration, respectively [21, 22, 23, 24]. With the ZnO sample, there was a Zn-O bond vibration band at 550-450 cm^{-1} [25]. In general, all the characteristic peaks of ZnO and g-C_3N_4 appeared in the spectra of ZCN. Combined with the XRD and FT-IR analysis, it reconfirmed the successful synthesis of the ZCN composite. The result showed a strong interaction between g-C_3N_4 and ZnO semiconductors.

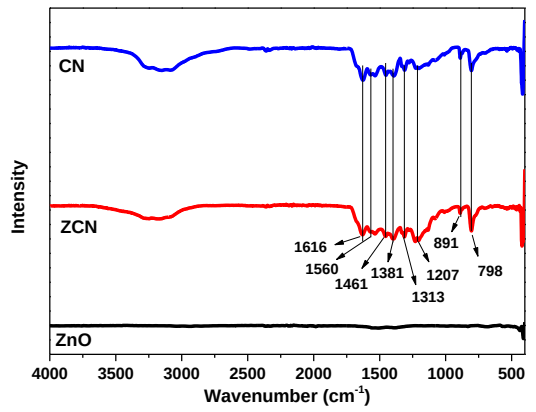

Fig.2. FT-IR spectra of ZnO, g-C_3N_4 and ZCN

The morphologies of the samples are indicated through SEM images. Fig. 3 illustrates the respective SEM photographs of ZnO, g-C_3N_4, and ZCN photocatalysts. The SEM image of g-C_3N_4 (Fig. 3) shows a typical multi-layered structure of graphitic carbon nitride corresponding to the in-plane structural packing pattern of tri-s -triazine building blocks. From Fig. 3, it is clear that the ZCN material has micropores with large diameters. The porosity observed in the ZCN nanocomposites is beneficial for enhanced photocatalysis due to the improvement of mass transport through the materials consisting of small elongated structures with a diameter of about 1µm [26]. These results further confirm the successful formation of the heterostructure of ZCN. The presence of elements such as Zn, O, C, and N in the composite mixture was determined by the EDS spectrum shown specifically in Fig.3.

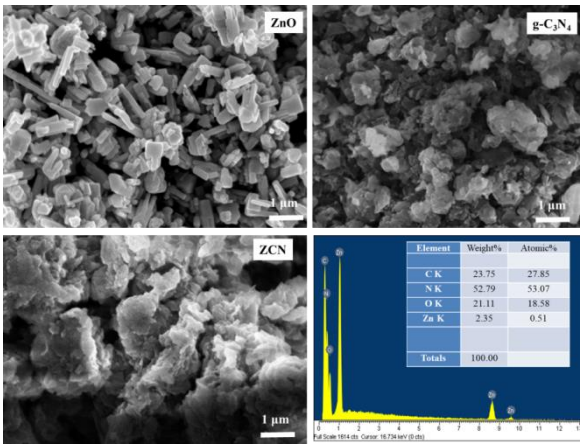

Fig. 3. FE-SEM images of ZnO, g-C_3N_4, ZCN, and EDS image of ZCN

UV-vis diffuse reflectance spectroscopy was carried out to investigate the optical properties of the samples. Fig.4 describes UV-vis diffuse reflectance spectra of g-C_3N_4, ZnO, and ZCN composite. The results from Fig.4 show a clear fundamental absorption edge of ZnO at 395 nm, and the band gap energy is determined to be 3.08 eV. Meanwhile, the main absorption edge of pure g-C_3N_4 occurs at a wavelength of about 445 nm and a band gap energy of 2.85 eV. As expected, compared with pure ZnO, the ZCN photocatalyst shows the same absorption edge, but the absorption extends to the visible light in the presence of g-C_3N_4. This result can be expected to be that the photocatalytic reaction of ZnO is improved under visible light irradiation when g-C_3N_4 is introduced into ZnO and leads to charge transfer between g-C_3N_4 and the valence band of ZnO.

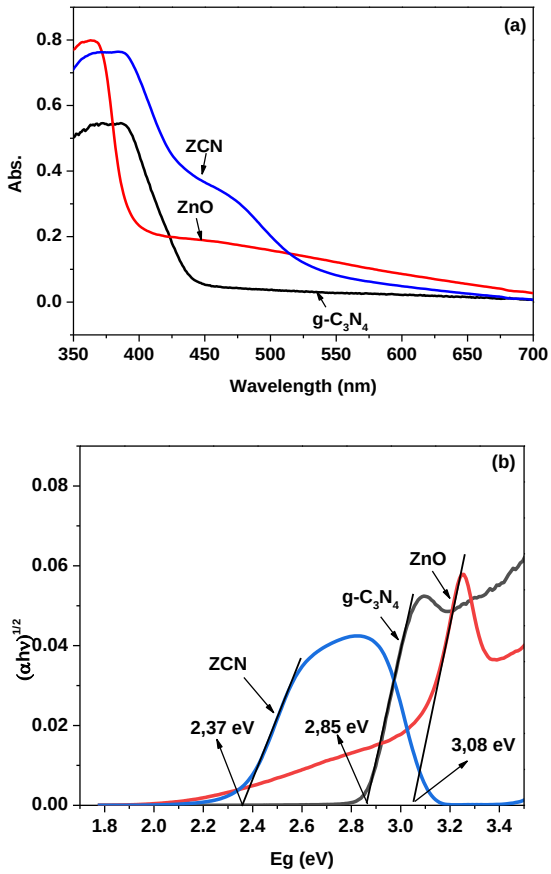

Fig. 4. UV-Vis-DRS spectra (a) and the plot of the Kubelka-Munk function for ZnO, g-C_3N_4, and ZCN (b).

3.2. Photocatalytic properties of materials

The photocatalytic activity of the decomposition of RhB solution (10 mg/L) by LED lamp 30W of materials is shown in Fig.5.

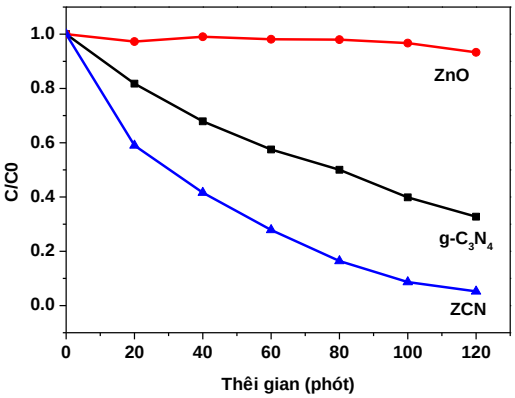

Fig. 5. Decolorization kinetics of RhB over ZnO, g-C_3N_4, and ZCN under visible light irradiation (conditions: $m_{catalyst}$ = 0.05 g; concentration of RhB = 10 mg/L; adsorption time = 30 min).

Before evaluating the catalytic activity, the material samples were adsorbed in the dark for 30 minutes to reach adsorption/desorption equilibrium. Fig. 5 shows that the ZCN sample exhibits higher photocatalytic activity to decompose RhB than the single ZnO and g-C_3N_4 after 120 minutes of illumination. Specifically, the photocatalytic efficiency of samples ZnO, g-C_3N_4, and ZCN is 6.68%, 67.27%, and 94.75%, respectively, while ZnO has almost no photocatalytic properties. The improved photocatalytic activity of the composite is due to the synergistic effect of ZnO and g-C_3N_4. The connection of two semiconductors (ZnO and g-C_3N_4) will form a heterojunction at the contact surface. And the formed heterojunctions are beneficial to the effective separation of charge carriers. The presence of g-C_3N_4 in the ZCN sample overcomes the disadvantage of photogenerated electron-hole recombination that occurs in individual semiconductor materials.

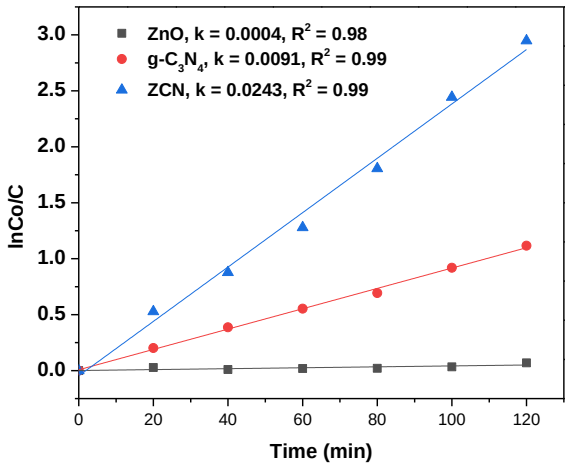

Fig. 6. Plot of Langmuir-Hinshelwood model of ZnO, g-C_3N_4, and ZCN materials.

The Langmuir-Hinshelwood model was employed to analyze the kinetics data in which the linear plot of $\ln(C_t/Co)$ vs.t is constructed. Fig. 6 presents the Langmuir-Hinshelwood plots of ZnO, g-C_3N_4, and ZCN materials. The high determination coefficients, R^2 (0.99–1), confirm that the kinetic degradation reaction of RhB over materials is fixed well in the Langmuir-Hinshelwood model.

The results show that the ZCN catalyst has the highest reaction rate (0.0243 min^{-1}), 2.76 times higher than g-C_3N_4, and much more significant than ZnO material. This indicates that adding g-C_3N_4 to ZnO significantly improved the photocatalytic activity of pure ZnO.

4. CONCLUSION

ZCN material is synthesized by a simple calcination method. This heterostructure shows the ability to effectively capture and store charge

in the visible light region, significantly improving the photocatalytic efficiency of the material in the decomposition of RhB in a water environment. The reaction follows a Langmuir-Hinshelwood model with a calculated rate constant of 0.0243 min^{-1}. The ZCN composite material exhibits good heterojunction between ZnO and g-C_3N_4 and is a promising semiconductor material for decomposing organic dyes in water solution by photocatalysis under visible light.

REFERENCES

1. Chai, S. Y.; Kim, Y. J.; Jung, M. H.; Chakraborty, A. K.; Jung, D.; Lee, W. I., Heterojunctioned BiOCl/Bi_2O_3, a new visible light photocatalyst. *Journal of Catalysis* **2009,** *262* (1), 144-149.

2. Tran Huu, H.; Thi, M. D. N.; Nguyen, V. P.; Thi, L. N.; Phan, T. T. T.; Hoang, Q. D.; Luc, H. H.; Kim, S. J.; Vo, V., One-pot synthesis of S-scheme MoS_2/g-C_3N_4 heterojunction as effective visible light photocatalyst. *Scientific Reports* **2021,** *11* (1), 14787.

3. Zhang, S.; Su, C.; Ren, H.; Li, M.; Zhu, L.; Ge, S.; Wang, M.; Zhang, Z.; Li, L.; Cao, X., In-situ fabrication of g-C_3N_4/ZnO nanocomposites for photocatalytic degradation of methylene blue: synthesis procedure does matter. *Nanomaterials* **2019,** *9* (2), 215.

4. Uma, R.; Ravichandran, K.; Sriram, S.; Sakthivel, B., Cost-effective fabrication of ZnO/g-C_3N_4 composite thin films for enhanced photocatalytic activity against three different dyes (MB, MG and RhB). *Materials Chemistry and Physics* **2017,** *201*, 147-155.

5. Liu, W.; Wang, M.; Xu, C.; Chen, S., Facile synthesis of g-C_3N_4/ZnO composite with enhanced visible light photooxidation and photoreduction properties. *Chemical Engineering Journal* **2012,** *209*, 386-393.

6. Guan, R.; Li, J.; Zhang, J.; Zhao, Z.; Wang, D.; Zhai, H.; Sun, D., Photocatalytic performance and mechanistic research of ZnO/g-C_3N_4 on degradation of methyl orange. *ACS omega* **2019,** *4* (24), 20742-20747.

7. Suhag, M. H.; Khatun, A.; Tateishi, I.; Furukawa, M.; Katsumata, H.; Kaneco, S., One-Step Fabrication of the ZnO/g-C_3N_4 Composite for Visible Light-Responsive Photocatalytic Degradation of Bisphenol E in Aqueous Solution. *ACS omega* **2023,** *8* (13), 11824-11836.

8. Wen, J.; Xie, J.; Chen, X.; Li, X., A review on g-C_3N_4-based photocatalysts. *Applied surface science* **2017,** *391*, 72-123.

9. Wang, K.; Li, Q.; Liu, B.; Cheng, B.; Ho, W.; Yu, J., Sulfur-doped g-C_3N_4 with enhanced photocatalytic CO_2-reduction performance. *Applied Catalysis B: Environmental* **2015,** *176*, 44-52.

10. Liu, E.; Chen, J.; Ma, Y.; Feng, J.; Jia, J.; Fan, J.; Hu, X., Fabrication of 2D SnS_2/g-C_3N_4 heterojunction with enhanced H_2 evolution during photocatalytic water splitting. *Journal of colloid and interface science* **2018,** *524*, 313-324.

11. Van Viet, P.; Nguyen, H.-P.; Tran, H.-H.; Bui, D.-P.; Pham, M.-T.; You, S.-J.; Thi, C. M., Constructing g-C_3N_4/SnO_2 S-scheme heterojunctions for efficient photocatalytic NO removal and low NO_2 generation. *Journal of Science: Advanced Materials and Devices* **2021,** *6* (4), 551-559.

12. Shi, L.; Zhou, Z.; Zhang, Y.; Ling, C.; Li, Q.; Wang, J., Photocatalytic conversion of CO to fuels with water by B-doped graphene/g-C3N4 heterostructure. *Science Bulletin* **2021,** *66* (12), 1186-1193.

13. Thi, T. H. N.; Huu, H. T.; Phi, H. N.; Nguyen, V. P.; Le, Q. D.; Thi, L. N.; Phan, T. T. T.; Vo, V., A facile synthesis of SnS_2/g-C_3N_4 S-scheme heterojunction photocatalyst with enhanced photocatalytic performance. *Journal of Science: Advanced Materials and Devices* **2022,** *7* (2), 100402.

14. Garg, R.; Gupta, R.; Bansal, A., Synthesis of g-C_3N_4/ZnO nanocomposite for photocatalytic degradation of a refractory organic endocrine disrupter. *Materials Today: Proceedings* **2021,** *44*, 855-859.

15. Ngullie, R. C.; Alaswad, S. O.; Bhuvaneswari, K.; Shanmugam, P.; Pazhanivel, T.; Arunachalam, P., Synthesis and Characterization of Efficient ZnO/g-[C. sub. 3][N. sub. 4] Nanocomposites Photocatalyst for Photocatalytic Degradation of Methylene Blue. *Coatings (Basel)* **2020,** *10* (5).

16. Zhu, B.; Xia, P.; Li, Y.; Ho, W.; Yu, J., Fabrication and photocatalytic activity enhanced mechanism of direct Z-scheme g-

C_3N_4/Ag_2WO_4 photocatalyst. *Applied Surface Science* **2017,** *391*, 175-183.

17. Li, X.; Li, M.; Yang, J.; Li, X.; Hu, T.; Wang, J.; Sui, Y.; Wu, X.; Kong, L., Synergistic effect of efficient adsorption g-C_3N_4/ZnO composite for photocatalytic property. *Journal of Physics and Chemistry of Solids* **2014,** *75* (3), 441-446.

18. Dulta, K.; Koşarsoy Ağçeli, G.; Chauhan, P.; Jasrotia, R.; Chauhan, P., Ecofriendly synthesis of zinc oxide nanoparticles by Carica papaya leaf extract and their applications. *Journal of Cluster Science* **2021**, 1-15.

19. Lotsch, B. V.; Döblinger, M.; Sehnert, J.; Seyfarth, L.; Senker, J.; Oeckler, O.; Schnick, W., Unmasking melon by a complementary approach employing electron diffraction, solid-state NMR spectroscopy, and theoretical calculations—structural characterization of a carbon nitride polymer. *Chemistry–A European Journal* **2007,** *13* (17), 4969-4980.

20. Liu, J.; Zhang, T.; Wang, Z.; Dawson, G.; Chen, W., Simple pyrolysis of urea into graphitic carbon nitride with recyclable adsorption and photocatalytic activity. *Journal of Materials Chemistry* **2011,** *21* (38), 14398-14401.

21. Nie, N.; Zhang, L.; Fu, J.; Cheng, B.; Yu, J., Self-assembled hierarchical direct Z-scheme g-C_3N_4/ZnO microspheres with enhanced photocatalytic CO_2 reduction performance. *Applied Surface Science* **2018,** *441*, 12-22.

22. Xing, C.; Wu, Z.; Jiang, D.; Chen, M., Hydrothermal synthesis of In_2S_3/g-C_3N_4 heterojunctions with enhanced photocatalytic activity. *Journal of colloid and interface science* **2014,** *433*, 9-15.

23. Jiang, D.; Chen, L.; Zhu, J.; Chen, M.; Shi, W.; Xie, J., Novel p–n heterojunction photocatalyst constructed by porous graphite-like C_3N_4 and nanostructured BiOI: facile synthesis and enhanced photocatalytic activity. *Dalton Transactions* **2013,** *42* (44), 15726-15734.

24. Hong, J.; Xia, X.; Wang, Y.; Xu, R., Mesoporous carbon nitride with in situ sulfur doping for enhanced photocatalytic hydrogen evolution from water under visible light. *Journal of Materials Chemistry* **2012,** *22* (30), 15006-15012.

25. Paul, D. R.; Gautam, S.; Panchal, P.; Nehra, S. P.; Choudhary, P.; Sharma, A., ZnO-modified g-C_3N_4: a potential photocatalyst for environmental application. *ACS omega* **2020,** *5* (8), 3828-3838.

26. Yuan, Z.-Y.; Su, B.-L., Insights into hierarchically meso–macroporous structured materials. *Journal of Materials Chemistry* **2006,** *16* (7), 663-677.